Carbohydrate Polymers 83 (2011) 1707–1714

Contents lists available at ScienceDirect

Carbohydrate Polymers

journal homepage: www.elsevier.com/locate/carbpol

Characterization of the inclusion complex of zerumbone with hydroxypropyl-β-cyclodextrin

Eltayeb E.M. Eid[a,b,**], Ahmad Bustamam Abdul[a,c,**], Fakhr Eldin O. Suliman[d,*], Mohd A. Sukari[e], A. Rasedee[f], Safa S. Fatah[a]

[a] MAKNA-UPM, Cancer Research Laboratory, Institute of Bioscience, University Putra Malaysia, Malaysia
[b] Laboratory of Immunotherapeutic and Vaccines (LIVES), Institute of Bioscience, University Putra Malaysia, Malaysia
[c] Department of Biomedical Science, Faculty of Medicine & Health Science, University Putra Malaysia, Malaysia
[d] Department of Chemistry, College of Science, Sultan Qaboos University, Box 36, Al Khod 23, Oman
[e] Department of Chemistry, Faculty of Science, University Putra Malaysia, Malaysia
[f] Department of Veterinary Pathology and Microbiology, Faculty of Veterinary Medicine, University Putra Malaysia, Malaysia

ARTICLE INFO

Article history:
Received 1 September 2010
Received in revised form 13 October 2010
Accepted 14 October 2010
Available online 20 October 2010

Keywords:
Zerumbone
Hydroxypropyl-β-cycoldextrin
Cytotoxicity
Molecular modeling
PM6

ABSTRACT

In this paper we investigated the inclusion complexation between zerumbone (ZER) and hydroxylpropyl-β-cyclodextrin (HPβCD) at four different temperatures: 293–318 °K. The thermodynamic parameters (ΔH, ΔS and ΔG) for the formation of the complex were obtained from the van't Hoff equation. The complex with HPβCD was characterized by differential scanning calorimetry (DSC), X-ray diffractometry (XRD), Fourier transform infrared spectroscopy (FT-IR), and molecular modeling using PM6. The solubility of ZER was enhanced >30 fold after complexation. Calculations show that ZER penetrates completely into the cavity of HPβCD. The complex retained its cytotoxic activity as shown by *in vitro* cell survival assay on human cervical cancer (Hela), breast cancer (MCF7 and MDA-MB 231) and human leukemic (CEMss) cell lines. HPβCD is, therefore, a suitable encapsular capable of forming thermodynamically stable complex with ZER for save delivery of the compound as an anticancer drug in the future.

1. Introduction

Cyclodextrins are cyclic oligosaccharides constituted by six (α-cyclodextrin), seven (β-cyclodextrin) and eight (γ-cyclodextrin) glucopyranose units linked by α-(1, 4) bonds (Szejtli, 1998). The form of cyclodextrin molecules resembles truncated cones with secondary hydroxyl groups located at the wider edge of the ring and the primary groups on the narrower edge having a different cavity volume. Their most popular feature is the marked difference of polarity between the internal and external surfaces: the inner part is made nonpolar by the glycosidic oxygens and methine protons, whereas the external surface is polar by virtue of the presence of secondary and primary hydroxyls on the large and small rims, respectively (Atwood, Davis, Macincol, & Vogtle, 1996; Khan, Forgo, Stine, & D'Souza, 1998). The cyclodextrin structure provides a molecule shaped like a segment of a hollow cone that is capable of forming stable, supramolecular structures with various molecules (Hazekamp & Verpoorte, 2006; Jullian, Miranda, Zapata-Torres, Mendizabal, & Olea-Azar, 2007; Liu & Zhu, 2006; Rajabi, Tayyari, Salari, & Tayyari, 2008; Sagiraju & Jursic, 2008; Spamer, Muller, Wessels, & Venter, 2002; Wang, Han, & Feng, 2007).

Hydroxypropyl-β-cyclodextrin (HPβCD) is a hydroxyalkyl β-cyclodextrin derivative that is widely studied in the field of drug encapsulation because of its inclusion ability as well as its high water solubility (Gould & Scott, 2005) and (Granero, Maitre, Garnero, & Longhi, 2008). In addition, toxicological studies pointed out that HP-βCD is well tolerated by the human body both by intravenous and oral administration (Fromming & Szejtli, 1996).

The World Health Organization estimated that 80% of the earth's inhabitants rely on traditional medicine for their primary health care needs, and most of this therapy involves the use of plant extracts or their active components (Craig, 1999). Worldwide considerable attention has been focused on herbal medicine which is based on the premise that these herbal plants may contain natural substances that can promote health and alleviate diseases. Twenty-five percent of modern drugs prescribed worldwide are plant-derived, where 121 of these active compounds are currently used in the treatment of various illnesses (Rates, 2001).

* Corresponding author. Tel.: +968 2414 1480; fax: +968 2414 1469.
** Corresponding authors at: MAKNA-UPM, Cancer Research Laboratory, Institute of Bioscience, University Putra Malaysia, Malaysia.
Tel.: +60 172810858; fax: +60 38946195.
E-mail addresses: chemisteltayeb@yahoo.com (E.E.M. Eid), abustamam@putra.upm.edu.my (A.B. Abdul), fsuliman@squ.edu.om (F.E.O. Suliman).

0144-8617/$ – see front matter © 2010 Elsevier Ltd. All rights reserved.
doi:10.1016/j.carbpol.2010.10.033

Zingiber zerumbet Smith locally known as 'lempoyang' wild ginger belongs to Zingiberaceae family. It is native to South East Asia but has been a widely cultivated plant in village gardens throughout the tropical and subtropical area around the world and has naturalized in some areas for its medicinal properties. *Z. zerumbet* is used in local traditional medicine as a cure for a number of illnesses. Scientific research towards *Z. zerumbet* proved that it contained a suppressive effect which was conducted by a bioactive compound, zerumbone (ZER) (Kinghorn et al., 1997; Koshimizu, Ohigashi, Tokuda, Kondo, & Yamaguchi, 1988). In some Southeast Asian countries, the rhizomes of the plant are employed as traditional medicines for anti-inflammation, while the young shoots and inflorescence are used as condiments.

ZER (Fig. 1) is a crystalline sesquiterpene available in abundant amount from the wild ginger, *Z. zerumbet* Smith. It has an interesting biological activity with its cross conjugated ketone in an 11-membered ring (Kitayama et al., 2003). It has been shown to be one of the most promising chemopreventive agents against colon and skin cancer (Nakamura et al., 2004). It was reported to suppress colonic tumour marker formation in rats and induces apoptosis in colon cancer cell lines. The compound was shown to inhibit the proliferation of human colonic adenocarcinoma cell lines in a dose-dependent manner, while the growth of normal human dermal and colon fibroblast was less affected (Nakamura et al., 2004). The compound has also been shown to be active *in vivo* against DES-induced mice Cervical Intraepithelial Neoplasia (CIN) (Abdul et al., 2008) and was further demonstrated to inhibit both azoxymethane-induced rat aberrant crypt foci and phorbol ester-induced papilloma formation in mouse skin a further indication of its efficacy to prevent colon and skin cancers (Murakami et al., 2004; Tanaka et al., 2001). Recently, Sung, Murakami, Oyajobi, & Aggarwal (2009) reported ZER as modulator for osteoclastogenesis induced by RANKL and breast cancer (Sung et al., 2009). In addition ZER was reported to effectively suppress mouse colon and lung carcinogenesis through multiple modulatory mechanisms (Kim et al., 2009).

In this work we investigated the interaction of ZER with HPβCD in aqueous media, aiming to enhance the solubility of ZER. This is an important physicochemical property required in the early stage of drug development. The phase solubility diagram was studied at different temperatures (293–318 K) using an HPLC technique with a photodiode array (PDA) detection system. Furthermore, the inclusion complex was characterized using FTIR, thermal analysis, and XRD techniques. Molecular modeling techniques using the semiempirical method PM6 were also used to explain the complexation mechanism of ZER with HPβCD.

2. Experimental

2.1. Materials

ZER was extracted in cancer research laboratory, Institute of Bioscience, University Putra Malaysia (UPM). HPβCD was purchased from sigma Aldrich (St.louis, MO). All the reagents and chemicals used were of analytical grade. Ultrapure water was used throughout the experiments.

2.2. Phase solubility study

Phase solubility studies were carried out according to the method described by Higuchi and Connors (Higuchi & Connors, 1965). An excess amount of ZER (10–14 mg) was mixed in a series of water solutions containing increasing amount of HPβCD (0–0.01 M), dispersing by vortex mixer for 2 min, and then oscillating by rotary shaker (Certomat® BS-1, Sartorius group, Germany) at 20–45° for 72 h. After equilibrium was achieved, the samples were filtered through 0.45 μm nylon filter (waters, USA) and appropriately diluted. The concentration of the dissolved ZER was determined by HPLC (waters, USA). The HPβCD did not interfere with HPLC measurements. The apparent stability constants, *K*, were calculated from the phase solubility diagram using Eq. (1):

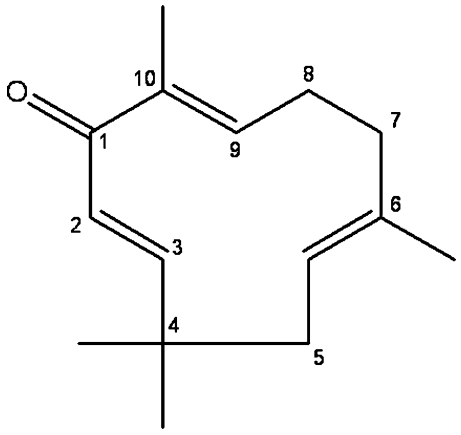

Fig. 1. Structure of zerumbone.

$$K = \frac{\text{slope}}{S_o(1 - \text{slope})} \quad (1)$$

where S_0 represents the intrinsic solubility of the drug.

2.3. Preparation of the inclusion complex

The inclusion complex was prepared by freeze drying method. Aqueous solutions containing zerumbone (ZER) and Hydroxypropyl-β-cyclodextrin (HPβCD) in 1:1 molar ratio was obtained by dissolving 0.2183 g ZER in 20 ml ultra-pure water containing 1.396 g HPβCD. The mixture was agitated in rotary shaker for 72 h at room temperature, then filtered through 0.45 μm filter and the clear solution was frozen at −80 °C, and subsequently freeze-dried for 24 h at −55 °C.

2.4. Preparation of physical mixture

The physical mixture of ZER and HPβCD in the same weight ratio as the lyophilized complex was prepared. The ZER and HPβCD were admixed in a mortar and pestle for 5 min to obtain a homogenous powder.

2.5. High performance liquid chromatography (HPLC)

The chromatographic system consists of a Waters Alliance (Milford, MA, USA) with a PDA detector (254 nm). The separation (10 μL injection volume) was carried out on C_{18} symmetry column (4.6 mm I.D. × 250 mm length, 5 μm particle size; Waters, Milford, MA, USA) maintained at ambient temperature. The mobile phases used for the analysis consisted of acetonitrile: methanol: 0.01 M potassium dihydrogen orthophosphate (50:40:10) delivered at a flow rate of 1 ml min^{-1}.

2.6. Differential scanning calorimetry (DSC)

DSC studies were performed to confirm the inclusion complex formation. Samples (HPβCD, ZER, physical mixture and inclusion complex) of about 2–4 mg were placed in a flat-bottomed aluminum pan and heated at a constant rate of 10 °C min^{-1} and

scanned using Mettler Toledo DSC822 (Swizterland) from approximately 20–120 °C under a constant flow of dry nitrogen.

2.7. Fourier transform infrared spectroscopy (FT-IR)

The FTIR spectra were recorded using VERTEX 70 FTIR (Ettlingen, Germany) using the potassium bromide (KBr) disc technique. The smoothing of the spectra and the baseline correction were applied. The FTIR measurements were performed in the scanning range of 4000–400 cm^{-1} at ambient temperature. The FT-IR spectra of the inclusion complexes were compared with their pure HβCD, ZER and physical mixture.

2.8. X-ray diffraction (XRD)

The powder samples were packed in the X-ray holder from the top prior to analysis. X-ray powder diffraction patterns were recorded on X-ray diffractometer, Phillips, using Cu-κα (λ = 1.5406 Å) radiation, voltage of 40 kV, and 30 mA current. The scanning rate employed was 2°/min over the range of 20–80°.

2.9. Molecular modeling

The initial geometries of zerumbone (ZER) and hydroxypropyl-β-CD (HPβCD) were optimized by PM6 using the MOPAC2009 package (http://www.openmopac.net) (Stewart, 1989). The β-cyclodextrin (βCD) structure was obtained from the crystallographic parameters provided by the Structural Data Base System of the Cambridge crystallographic Data Center (Aree & Chaichit, 2002, 2003). The structure of HPβCD was built by adding hydroxypropyl substituents to the βCD followed by optimization of the structure using PM6 level of theory. The inclusion complexes were constructed from the separately optimized cyclodextrin and the optimized structure of ZER. The starting geometries were constructed using CS Chem 3D Ultra (Version 8.0, Cambridgesoft.com) and were fully optimized with the PM6 method. The coordinate system used to define the process of complexation is based on placing the glycosidic oxygen atoms of the cyclodextrin onto the XY plane with their centre defined as the centre of the coordination system. Two different inclusion orientations were considered. In the first orientation (model A) ZER docked into the wider rim of the cyclodextrin by placing the oxygen atom of the carbonyl group coincident with the *Z*-axis. While in the second orientation (model B) ZER was docked into the wider rim of the cyclodextrin with the face that contains C7 of the molecule (Fig. 1) and by placing C7 coincident with the *Z*-axis. Multiple starting positions were generated by moving ZER molecule towards HPβCD along the *Z*-axis. The relative position of the host and the guest are measured by the position of the C1 for model A and by the position of C7 for model B. The inclusion complexes were emulated by moving the guest molecule from 13 to −7 Å, at 1 Å intervals. The complexation energy ΔE_{comp} is calculated for the minimum energy structures by the following equation:

$$\Delta E_{comp} = E_{comp} - E_{guest} - E_{host} \quad (2)$$

where, E_{comp}, E_{guest}, and E_{host} represents the total energy of the complex, of the free guest molecule and the free host molecule obtained by PM6 method, respectively. The magnitude of the energy change would be an indication of the driving force towards complexation. The more negative the complexation energy change is the more thermodynamically favourable is the inclusion complex.

2.10. Cell culture

Human cervical cancer cells (HeLa) and breast cancer cells (MCF7 and MDA-MB 231) were obtained from ATTC and leukemic cells (CEMss) were obtained from NIH. These were grown in RPMI 1640 supplemented with 10% fetal bovine serum, 1% penicillin-streptomycin and 1% amphotericin B. Flasks containing cells were incubated in a humidified incubator with 5% CO_2, at 37 °C. Cultures were frequently examined under inverted microscope (Micros, Austria).

2.11. Cytotoxicity assay

A stock solution of ZER in inclusion complex was prepared and was diluted to concentrations of 4–120 μg ml^{-1} with RPMI 1640. Cells were washed three times with 7 ml of PBS. Two and half millilitres of trypsin was added to the cells and incubated for 5 min in a CO_2 incubator. Once the cells were detached from the flask, 10 ml of RPMI with 10% FBS was added into the flask. Cell density was determined using a hemocytometer. Two hundred microlitres of cell suspension was placed in each well of 96 well plates at a concentration of 5×10^4 cells ml^{-1}. After 24 h of incubation, the content of each well was decanted and cells were treated with different concentrations of ZER in DMSO or in the presence of HβCD. The cells were incubated in CO_2 incubator at 37 °C for 3 days (72 h). Fifty microlitres of 5 mg ml^{-1} MTT (Micro culture Tetrazolium) solution was added into each well. The plate was covered with aluminum foil and incubated at 37 °C (5% CO_2) for 4 h in the dark to allow the active live cells to convert water-soluble yellow MTT solution into water insoluble purple formazan. After 4 h of incubation, the media containing MTT solution was aspirated. The remaining purple formazan was dissolved by adding 100 μl DMSO into each well and the absorbance was measured at 570 nm using an ELISA plate reader. This colorimetric assay is based on the ability of live and metabolically unimpaired tumour-cell targets to reduce MTT to a blue formazan product (Skehan, Storeng, & Scuderio,1990). The IC_{50} value (Concentration at which 50% of the cells are viable and the other 50% are killed) was determined from the dose-response curve (% cell viability versus concentration of ZER in DMSO or in inclusion complex).

3. Results and discussion

3.1. Phase solubility

The solubility diagram is useful for explaining inclusion complexation of poorly soluble compounds with cyclodextrins as a host in water because it gives not only the solubilizing ability of host but also the stability constant of the complexes by analyzing the solubility curves (Higuchi & Connors, 1965). Fig. 2 shows the phase solubility diagrams of ZER with HPβCD in water obtained at different temperatures. Clearly, the solubility of ZER increases linearly with the increase in the molar concentration of HPβCD. Fig. 2 shows a positive deviation from linearity at high cyclodextrin concentration therefore this system can be classified to follow an A_p type solubility diagram. The apparent stability constant ($K_{1:1}$) of the inclusion complex can be calculate from the linear fit of the curve and using Eq. (1). The calculated $K_{1:1}$ values at different temperatures range from 2600 to 8800 M^{-1} suggesting the formation of a favourable inclusion complex. The solubility of ZER in water is 0.0053 mM and was observed to increase to 0.173 mM in the presence of 0.01 M HPβCD at 20 °C. Clearly, the formation of an inclusion complex between ZER and HPβCD resulted in a great increase in solubility. The complexation efficiency (CE), is defined as the ratio of the concentration of the dissolved complex to the concentration of the dissolved free cyclodextrin and is used to evaluate the solubilization of drugs in cyclodextrins (Loftsson, Hreinsdóttir, & Másson, 2007). Using the phase solubility diagram we determined CE for the ZER-HPβCD to be 1.04,

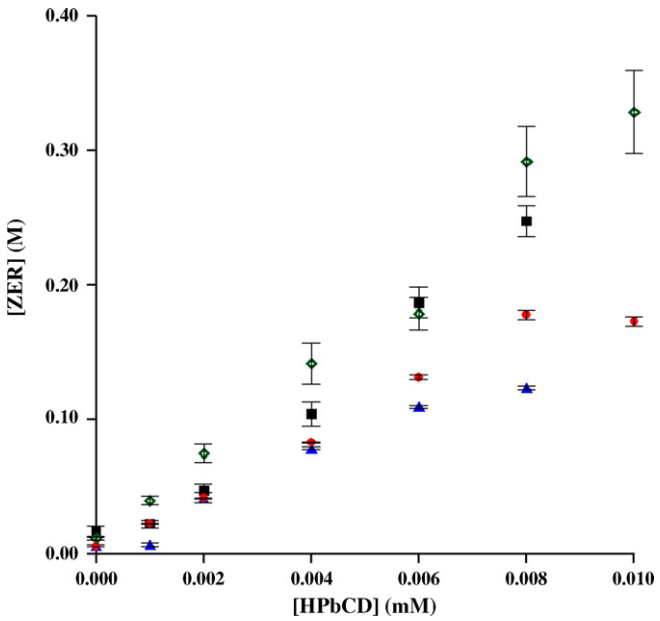

Fig. 2. Phase solubility diagram for the HPbCD-ZER host quest system at -▲-, 293 K; -●-, 303 K; -■-, 310 K; -◊-, 318 K.

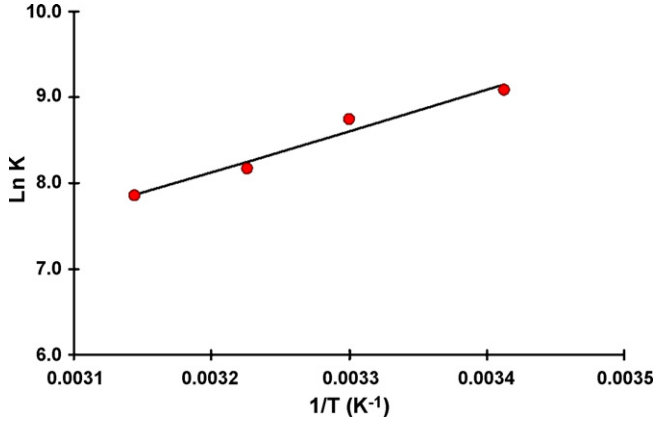

Fig. 3. The relationship between ln K_f and $1/T$ for ZER-HPβCD complex.

suggesting that HPβCD can be used in the formulation of this drug.

The Van't Hoff plot for the complex of ZER-HPbCD complex exhibited a linear relationship for ln K_f verus the inverse of the absolute temperature as shown in Fig. 3. The enthalpy change (ΔH), the entropy change (ΔS), and the Gibbs free energy change (ΔG) were calculated and the results are shown in Table 1. The negative values of ΔH indicate that the interaction processes between ZER and HPβCD are exothermic. ΔH is relatively high and could be related to the typical high energy of interactions such as van der Waals and hydrophobic interactions. These interactions originate from the penetration of hydrophobic guests into the cyclodextrin cavity as well as from the dehydration of the guest molecules (Lipkowitzv, 1998). The enthalpy of inclusion depends largely on the stabilization of the complexation and on the release of the water molecules that participate in the solvation of the nonpolar guest molecule (Rekharsky & Inoue, 1998). Therefore, the higher these interactions the higher are the stabilization of the guest–host complexes. The entropy change, ΔS, is also negative in these processes indicating that inclusion of ZER inside the nanocavity of HPβCD causes a decrease in the translational and the rotational degrees of freedom of the encapsulated molecules, and a more ordered system is thereby obtained. These results confirm further that the inclusion of ZER with HPβCD has occurred. Additionally, the negative value of ΔG is clear evidence that the inclusion process is spontaneous.

Table 1
The effect of temperature on K_f, ΔH, ΔS and ΔG of the inclusion complex of ZER-HPβCD.

T (K)	K_f (L mol^{-1})	ΔS (J mol^{-1} K^{-1})	ΔH (kJ mol^{-1})	ΔG (kJ mol^{-1})
293	8813	−59.8	−40.0	−22.4
303	6284	−59.8	−40.0	−21.9
310	3529	−59.8	−40.0	−21.5
318	2572	−59.8	−40.0	−21.0

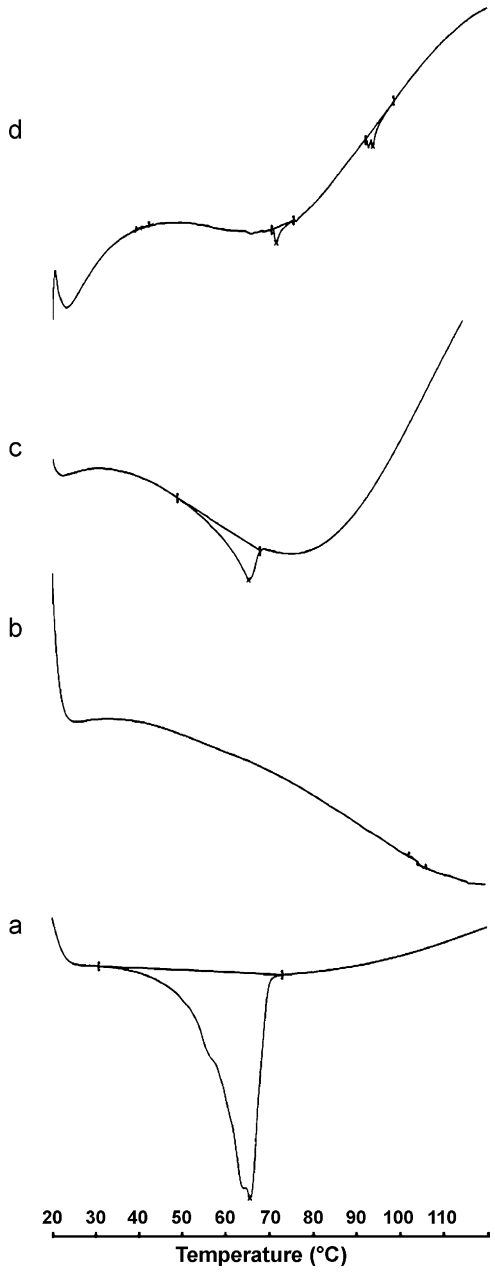

Fig. 4. DSC plots: (a) ZER, (b) HPβCD, (c) physical mixture, (d) inclusion complex.

3.2. Differential scanning calorimetry (DSC)

The DSC results presented in Fig. 4 demonstrate an endothermic peak for ZER at 65.3 °C which correspond to the melting point

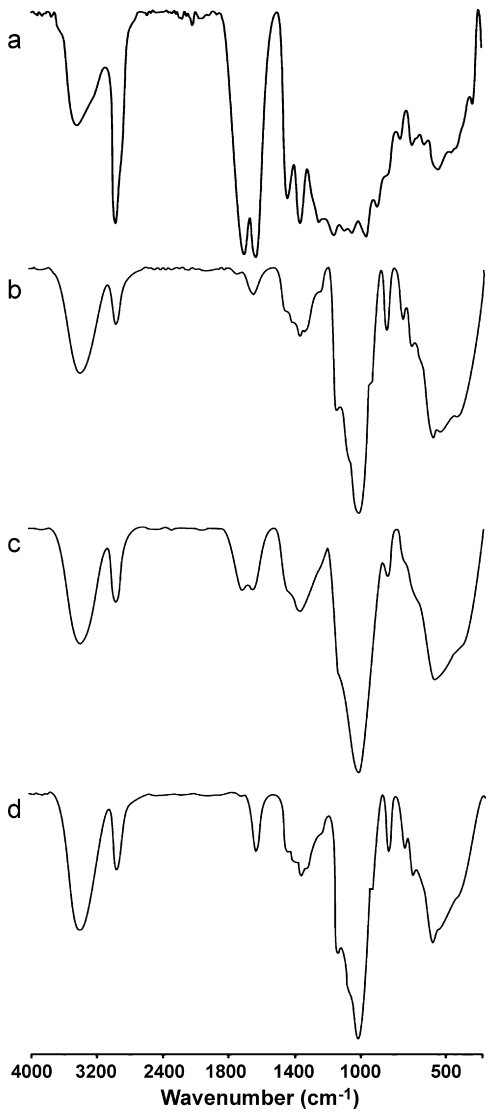

Fig. 5. FTIR of (a) ZER, (b) HPβCD, (c) physical mixture, (d) inclusion complex.

of ZER. The endothermic peak of ZER disappeared completely in the DSC thermogram of the inclusion complex as can be seen from Fig. 4. This explains the amorphous solid dispersion and the molecular encapsulation of ZER into the HPβCD nanocavity (Mura et al., 1999). On the other hand, the endothermic peak of ZER is observed in the physical mixture, but with marked broadening of less intensity (Fig. 4c). The observed broadening indicates the masking of ZER melting endotherm or the fusion between ZER melting and HPβCD decomposition due to the overlapping of the vicinity of the two effects, a similar phenomenon has been reported by (Liu, Qui, Gao, & Jin, 2006) Additionally, the significant reduction in intensity of the melting peak in the aforementioned systems is a clear indication of the low ZER to HPβCD molar ratio (1:1). Therefore, the existence of the ZER melting peak in the physical mixture could suggest that no true inclusion complex is formed in this system.

3.3. Fourier transform infrared spectroscopy (FT-IR)

FT-IR spectra of the ZER-HPβCD complex and those for pure compounds as well as the physical mixture are shown in Fig. 5. The characteristic IR peaks of ZER alone over the frequency range 500–4000 cm^{-1} occurred at 1655 cm^{-1}, for an α, β-unsaturated ketone and ethylenic linkage. The peaks at 1385 cm^{-1} and 1366 cm^{-1} indicates a gem dimethyl group. Whereas, the peaks at 1438, 1378, 919 cm^{-1} were due to the C=C groups, and the peak near 2946 cm^{-1} resulted from CH_2 stretching vibration. The broad peak in the ZER spectra at 3285 cm^{-1} is due to an OH stretching vibration probably originating from the residual water. Contributions to this band from the enol from of ZER are also possible. The cyclodextrin (HPβCD) showed clear peaks at 3300, 1638, 1035 and 564 cm^{-1}. However, all these peaks were shifted to lower frequency in the spectra of the inclusion complex, accompanied by the disappearance of all peaks of ZER from the inclusion complex spectra. The observed changes in the IR spectra of the drug complexed with HPβCD are due to the restriction of the vibration of ZER molecule upon encapsulation into HPβCD cavity. This is further associated with the breakdown of the intermolecular hydrogen bonding within the ZER molecule and the establishment of a less weak force in the complex system. Moreover, the observed decrease in the intensity of the carbonyl group of ZER may have resulted from its restriction upon inclusion within the HPβCD cavity.

3.4. X-ray diffraction (XRD)

The complexation of ZER with HPβCD was further investigated by XRD. X-ray powder diffraction patterns (XRD) of pure ZER, HPβCD, physical mixture and the corresponding inclusion complexes are shown in Fig. 6. There is no obvious peak in the X-ray diffraction spectrum of pure HPβCD as evidenced from the absence of diffraction peaks. In the X-ray diffractograms of ZER, sharp diffraction peaks were obtained, indicating the crystalline state of the drug. The same peaks appear clearly in the physical mixture, but with less intensity. In contrast, in the complex form we observed a diffraction pattern completely diffuse, which reveals its amorphousness. Lack of crystallinity is an added evidence for the formation of the inclusion complex (Williams, Mahaguna, & Sriwongjanya, 1998). This behaviour is indicative of the presence of an interaction between ZER and HPβCD that leads to the formation of a new solid phase (Moyano, Gines, Arias, & Rabasco, 1995; Williams et al., 1998) X-ray diffraction patterns of ZER-HPβCD system were characterized by large diffraction peaks; however there is no possibility to distinguish the characteristic peaks of pure crystalline ZER or HPβCD. These results indicate that ZER is no longer present as a crystalline material, and its HPβCD solid complexes exist in the amorphous state (Fig. 6d). The formation of an amorphous state proves that ZER was dispersed in a molecular state within HPβCD (Figueiras, Ribeiro, Vieira, & Veiga, 2007; Mukne & Nagarsenker, 2004).

3.5. Molecular modeling

To further scrutinize the mechanism of complexation between ZER and HPβCD we performed theoretical calculations using the semiempirical method PM6 (Stewart, 1989). Initially, using molecular mechanics, we observed that the energy of the complexes decreases as the guest molecule (ZER) enters into the HPβCD nanocavity in the two models. The energy was observed to increase again when the guest molecule leaves the cyclodextrin cavity. Interestingly, the variation of the energy of the system with respect to ZER entrance is the same for both models. After this initial procedure, the structures of the complexes obtained with the lowest energies were further optimized using the semiempirical PM6 method. The energy minimization using this method was performed without exerting any constraints.

From the PM6 calculated results (Table 2) we observed that the energy of the complex is always lower than that of the sum of the energies of the isolated guest and host molecules indicating the for-

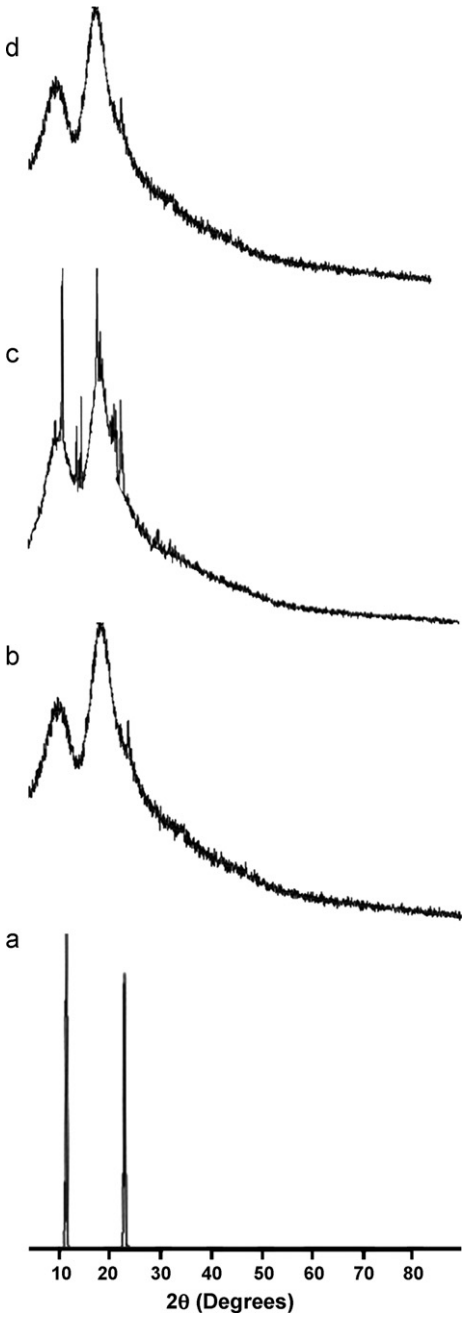

Fig. 6. Powder X-ray diffractogram: (a) ZER, (b) HPβCD, (c) physical mixture, (d) inclusion complex.

Table 2
Interaction energies and thermodynamic properties of ZER-HPβCD inclusion complexes.

Method	Parameter	Inclusion complex	
		Model A	Model B
PM6 (vacuum)	ΔE (kJ mol^{-1})	−75.9	−49.8
	ΔH (kJ mol^{-1})	−86.8	−57.9
	ΔG (kJ mol^{-1})	44.0	−62.5
	ΔS (J mol^{-1} K^{-1})	−439	−404
PM6 (aqueous)	ΔE (kJ mol^{-1})	−48.7	−47.3
	ΔH (kJ mol^{-1})	−55.7	−52.7
	ΔG (kJ mol^{-1})	53.0	46.0
	ΔS (J mol^{-1} K^{-1})	−365	−331

In vacuum: E_{ZER} = −100.7.1 kJ mol^{-1}, $E_{HP\beta CD}$ = −6695.8. In aqueous media: E_{ZER} = −167.5.1 kJ mol^{-1}, $E_{HP\beta CD}$ = −7111.2.

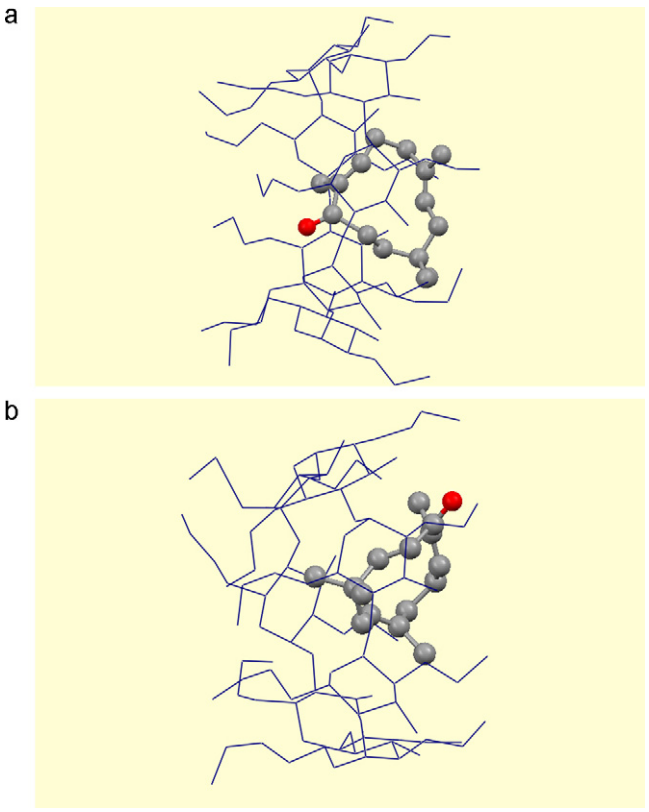

Fig. 7. Optimized structures of HPβCD-ZER complex in two orientations by PM6 semiempirical method: (a) model A and (b) model B.

mation of favourable complexes in both models. The binding energy of model A complex in vacuum is 26.1 kJ mol^{-1} lower than that of model B suggesting that the molecule enters the cyclodextrin cavity via the carbonyl group. In the aqueous phase, the difference in stabilization energy becomes negligible between the two models compared with that in the vacuum; however the orientation of the complex adopted by model A is still favoured. The optimized guest–host structures for binding of ZER with HPβCD in both orientations obtained by PM6 calculations are shown in Fig. 7. These figures clearly show that ZER is completely included into the cyclodextrin cavity, which may explain the greater enhanced solubility of ZER upon addition of HPβCD.

To further investigate the thermodynamics of the binding of ZER by HPβCD, we run statistical thermodynamics calculations at 1 atm and 298.15 K in vacuum and in water by PM6 methods. The thermodynamic quantities of the complexation process, such as enthalpy change (ΔH), the thermal Gibbs free energy change (ΔG) and the entropy change (ΔS) were all calculated and are given in Table 2. It is observed from this table that the complexation of ZER with HPβCD is exothermic as evidenced by the negative enthalpy changes obtained. Furthermore, the enthalpy change for the inclusion complexes of ZER with HPβCD is more negative for model A indicating a stronger interactions between ZER and the cyclodextrin in this orientation. Both models were obtained with comparable enthalpies, however, model A is more stable than model B by 3 kJ mol^{-1}. The enthalpy changes calculated by PM6 agree well with those obtained experimentally (−40.0 kJ mol^{-1}). This suggests that the PM6 calculated structures and energy describes the system efficiently. However, the calculated entropy changes for the complexation of ZER with HPβCD is different than the experimentally obtained entropy change (−59.8 J K^{-1}mol^{-1}). As a result the calculated Gibbs free energy also deviated greatly from the experimental one (−22.4 kJ mol^{-1}). The main factors that

contribute to the complexation thermodynamics of cyclodextrins also include the release of water molecules from the cycoldextrin cavity and the conformational changes of cyclodextrin molecules that occur due to the complexation (Lipkowitzv, 1998; Rekharsky & Inoue, 1998). On the other hand, the disruption of water clusters around the guest in the aqueous phase is also an important factor that contributes significantly to the stabilization of guest–host interactions. This is usually accompanied by a substantial increase in entropy and as a result contributes significantly to the stabilization of the inclusion complexes. Therefore, the greater difference in entropy values may have originated from the neglect of the hydrophobic effect resulting from the disruption of the water molecules during the inclusion process.

3.6. Cytotoxicity assay

Growth-inhibition and cytotoxic activities of ZER dissolved in an organic solvent and ZER-HPβCD inclusion complex against a human adenocarcinoma cervical cancer (HeLa) and breast cancer (MCF-7 and MDA-MB 231) cell lines and leukemic cancer cell lines (CEMss) were investigated. The IC_{50} values of the plain ZER against the four tested cell lines were (10.3 ± 2.40, 13.00 ± 4.5, 14.30 ± 3.9 and 9.10 ± 2.30 μg/ml) for Hela, MCF7, MDA-MB 231 and CEMss, 12, respectively, while the IC_{50} values of the ZER-HPβCD inclusion complex were 13.0 ± 3.15, 16.0 ± 4.30, 17.0 ± 4.50 and 11.50 ± 6.70 for Hela, MCF7, MDA-MB 231 and CEMss, respectively. When comparing the ZER and ZER-HPβCD inclusion complex, there was no difference between the two formulations as the differences in the cytotoxic effects were not significant. For all cell lines tested the similarity in cytotoxicity of both ZER and ZER-HPβCD inclusion complex was confirmed by the IC_{50} values. It has been observed that all formulations exerted very similar cytotoxic effects against all the tested cell lines after a 72-h incubation time. Cell viability data is demonstrative of the anticancer efficacy of ZER-loaded HPβCD inclusion complex, which is similar to, and slightly higher than that of a plain ZER solution in organic solvents.

4. Conclusion

Inclusion complex of ZER and HPβCD was prepared in aqueous solutions at four different temperatures (293–318 K). The formation of the inclusion complex was characterized by DSC, FT-IR, XRD, and molecular modeling using PM6 semiempirical method. All the characterization results show that ZER fits well inside the nanocavity of HPβCD. Taking into account these results, we conclude that the complexation of ZER with HPβCD, can lead to important modifications of the physicochemical properties (solubility, stability, bioavailability) of guest molecule. These results indicate that this drug is now ready for biopharmaceutical characterization that would further lead to preclinical studies of ZER as a potential candidate for the treatment of cancer.

Acknowledgements

The authors would like to appreciate the support from University Putra Malaysia (RUGS 91143), the Laboratory of Immunotherapeutic and Vaccines (LIVES), Institute of Bioscience UPM, and The National Cancer Council Malaysia (MAKNA) (grants IRPA No: 06-02-04-0720-EA001). Mr. Mohd. Hanif. MD. Arshad's technical assistance is greatly acknowledged.

References

Abdul, A. B., Al-Zubairi, A. S., Devi, N. D., Wahab, S. I., Zain, Z. N., Ruslay, S., et al. (2008). Anticancer activity of natural compound (ZER) extracted from *Zingiber zerumbet* in human Hela cervical cancer cells. *International Journal of Pharmacology*, *4*, 160–168.

Aree, T. N., & Chaichit, N. (2002). Crystal structure of β-cyclodextrin–dimethyl sulfoxide inclusion complex. *Carbohydrate Research*, *337*, 2487–2494.

Aree, T. N., & Chaichit, N. A. (2003). A new crystal form of β-cyclodextrin–ethanol inclusion complex: channel-type structure without long guest molecules. *Carbohydrate Research*, *338*, 1581–1589.

Atwood, J. L., Davies, J. E., Macnicol, D., & Vogtle, F. (1996). *Comprehensive supramolecular chemistry* UK: Pergamon Press.

Craig, W. J. (1999). Health-promoting properties of common herbs. *American Journal of Clinical Nutrition*, *70*, 491S–499S.

Figueiras, A., Ribeiro, L., Vieira, M., & Veiga, F. (2007). Preparation and physicochemical characterization of omeprazole:methyl-β-cyclodextrin inclusion complex in solid state. *Journal of Inclusion Phenomena and Macrocyclic Chemistry*, *57*, 173–177.

Fromming, K. H., & Szejtli, J. (1996). Pharmacokinetics and toxicology of cyclodextrins. In J. Szejtli, & L. Szente (Eds.), *Proceedings of the 8th international symposium on cyclodextrins* (pp. 33–45).

Gould, S., & Scott, R. C. (2005). 2-Hydroxypropyl-β-cyclodextrin (HP-β-CD): a toxicology review. *Food and Chemical Toxicology*, *43*, 1451–1459.

Granero, G. E., Maitre, M. M., Garnero, C., & Longhi, M. R. (2008). Synthesis, characterization and in vitro release studies of a new acetazolamine–HP-β-CD-TEA inclusion complex. *European Journal of Medicinal Chemistry*, *43*, 464–470.

Hazekamp, A, & Verpoorte, R. (2006). Structure elucidation of the tetrahydrocannabinol complex with randomly methylated β-cyclodextrin. *European Journal of Pharmaceutical Sciences*, *29*, 340–347.

Higuchi, T., & Connors, K. A. (1965). Phase solubility techniques. *Advances in Analytical Chemistry and Instrumentation*, *4*, 117–212.

Jullian, C., Miranda, S., Zapata-Torres, G., Mendizabal, F., & Olea-Azar, C. (2007). Studies of inclusion complexes of natural and modified cyclodextrin with (+) catechin by NMR and molecular modelling. *Bioorganic & Medicinal Chemistry*, *15*, 3217–3224.

Khan, A. R., Forgo, P., Stine, K. J., & D'Souza, V. T. (1998). Methods for selective modifications of cyclodextrins. *Chemical Reviews*, *98*, 1977–1996.

Kim, M., Miyamoto, S., Yasui, Y., Oyama, T., Murakami, A., & Tanaka, T. (2009). Zerumbone, a tropical ginger sesquiterpene, inhibits colon and lung carcinogenesis in mice. *International Journal of Cancer*, *124*, 264–271.

Kinghorn, A. D., Fransworth, N. R., Soejarto, D. D., Cordell, G. A., Pezzuto, J. M., Udeani, G. O., et al. (1997). Novel strategies for the discovery of plant derived anticancer agents. *Pure and Applied Chemistry*, *71*, 1611–1618.

Kitayama, T., Yokoi, T., Kawai, Y., Hill, R. K., Morita, M., Okamoto, T., et al. (2003). The chemistry of zerumbone. Part 5: Structural transformation of the dimethylamine derivatives. *Tetrahedron*, *59*, 4857–4866.

Koshimizu, K., Ohigashi, H., Tokuda, H., Kondo, A., & Yamaguchi, K. (1988). Screening of edible plants against antitumor promoting activity. *Cancer Letters*, *39*, 24757.

Lipkowitzv, K. B. (1998). Applications of computational chemistry to the study of cyclodextrins. *Chemical Reviews*, *98*, 1829–1874.

Liu, J., Qiu, L., Gao, J., & Jin, Y. (2006). Preparation, characterization and in vivo evaluation of formulation of baicalein with hydroxypropyl-β cyclodextrin. *International Journal of Pharmaceutics*, *312*, 137–143.

Liu, L. X., & Zhu, S. Y. (2006). Preparation and characterization of inclusion complexes of prazosin hydrochloride with β-cyclodextrin and hydroxypropyl-β-cyclodextrin. *Journal of Pharmaceutical and Biomedical Analysis*, *40*, 122–127.

Loftsson, T., Hreinsdóttir, D., & Másson, M. (2007). The complexation efficiency. *Journal of Inclusion Phenomena and Macrocyclic Chemistry*, *57*, 545–552.

Moyano, J. R., Gines, J. M., Arias, M. J., & Rabasco, A. M. (1995). Study of the dissolution characteristics of oxazepam via complexation with β-cyclodextrin. *International Journal of Pharmaceutics*, *14*, 95–102.

Mukne, A. P., & Nagarsenker, M. S. (2004). Triamterene-b-cyclodextrin systems: preparation, characterization and in vivo evaluation. *AAPS Pharmaceutical Science and Technology*, *5*, 83–90.

Mura, P. E., Adragna, Rabasco, A. M., Moyano, J. R., Pérez-Martinez, J. I., Arias, M. J., et al. (1999). *Drug Development and Industrial Pharmacy*, *25*, 279.

Murakami, A., Tanaka, T., Lee, J. Y., Surh, Y. J., Kim, H. W., Kawabata, K., et al. (2004). Zerumbone, a sesquiterpene in subtropical ginger, suppresses skin tumour initiation and promotion stages in ICR mice. *International Journal of Cancer*, *110*, 481–490.

Nakamura, Y., Chiho, Y., Murakami, A., Ohigashi, H., Osawa, T., & Uchida, K. (2004). Zerumbone, a tropical ginger sesquiterpene, activates phase II drug metabolizing enzymes. *FEBS Letters*, *572*, 245–250.

Rajabi, O., Tayyari, F., Salari, R., & Tayyari, S. F. (2008). Study of interaction of spironolactone with hydroxypropyl-β-cyclodextrin in aqueous solution and in solid state. *Journal of Molecular Structure*, *878*, 78–83.

Rates, S. M. K. (2001). Plants as source of drugs. *Toxicon*, *39*, 603–613.

Rekharsky, M. V., & Inoue, Y. (1998). Complexation thermodynamics of cyclodextrins. *Chemical Reviews*, *98*, 1875.

Sagiraju, S., & Jursic, B. S. (2008). NMR spectroscopic study of cyclodextrin inclusion complexes with A-007 prodrugs. *Carbohydrate Research*, *343*, 1180–1190.

Skehan, P., Storeng, R., & Scuderio, G. (1990). New colorimetric cytotoxicity assay for anticancer drug screening. *Journal of the National Cancer Institute*, *82*, 1107–1112.

Spamer, E., Muller, D. G., Wessels, P. L., & Venter, J. P. (2002). Characterization of the complexes of fluorosemide with 2-hydroxypropyl-β-cyclodextrin and sul-

fobutyl ether-7-β-cyclodextrin. *European Journal of Pharmaceutical Sciences*, *16*, 247–253.

Stewart, J. J. P. (1989). Optimization of parameters for semiempirical methods. I: Method. *Journal of Computational Chemistry*, *10*, 209–220.

Sung, B., Murakami, A., Oyajobi, B. O., & Aggarwal, B. B. (2009). Zerumbone abolishes RANKL-induced NF-κB activation, inhibits osteoclastogenesis, and suppresses human breast cancer induced bone loss in athymic nude mice. *Cancer Research*, *69*, 1477–1484.

Szejtli, J. (1998). Introduction and general overview of cyclodextrin chemistry. *Chemical Reviews*, *98*, 1743–1753.

Tanaka, T., Shimizu, M., Kohno, H., Yoshitani, S., Tsukio, Y., Murakami, A., et al. (2001). Chemoprevention of azoxymethane-induced rat aberrant crypt foci by dietary zerumbone isolated from *Zingiber zerumbet*. *Life Sciences*, *69*, 1935–1945.

Wang, H. Y., Han, J., & Feng, X. G. (2007). Spectroscopic study of orange G-β-cyclodextrin complex and its analytical application. *Spectrochimica Acta*, *66*, 578–585.

Williams, R. O., Mahaguna, V., & Sriwongjanya, M. (1998). Characterization of an inclusion complex of cholesterol and hydroxypropyl-β-cyclodextrin. *European Journal of Pharmaceutics Biopharmaceutics*, *46*, 355–360.